ADVANCED MATERIALS
www.advmat.de

Chirality Dependent Charge Transfer Rate in Oligopeptides

*Francesco Tassinari, Dilhara R. Jayarathna, Nirit Kantor-Uriel, Kathryn L. Davis, Vaibhav Varade, Catalina Achim, and Ron Naaman**

It is shown that "spontaneous magnetization" occurs when chiral oligopeptides are attached to ferrocene and are self-assembled on a gold substrate. As a result, the electron transfer, measured by electrochemistry, shows asymmetry in the reduction and oxidation rate constants; this asymmetry is reversed between the two enantiomers. The results can be explained by the chiral induced spin selectivity of the electron transfer. The measured magnetization shows high anisotropy and the "easy axis" of magnetization is along the molecular axis.

Biomolecules, among them oligopeptides and proteins, are suggested as material for self-assembled electronic and sensing devices.[1,2] Specifically, self-assembled organic monolayers on gold are a very popular tool for studying charge transfer through molecules.[3–5] Typically, the system includes a redox group attached to the tail of the adsorbed molecules of interest. The charge transfer between this group and the substrate is monitored either optically, using lasers,[6] or by electrochemistry.[7] It is almost natural to assume that the gold substrate and the redox group do not change their properties upon assembly. However, past experiments indicated that the simple description of gold surface, bridge organic molecule, and redox group as independent components is not complete and new properties may emerge when the three components are connected. For example, several groups reported that gold may show magnetic properties when molecules are self-assembled on its surface.[8–13] The magnetic properties were explained as resulting from both Pauli and orbital paramagnetism in the gold.[14] Furthermore, spin-dependent electron transfer was found when a monolayer of organic molecules containing paramagnetic atoms was adsorbed on gold, which indicates that the gold is magnetized.[15] The magnetic properties of gold may influence the electron transfer through the self-assembled monolayer of chiral molecules. In recent years it was established that electron transfer through chiral systems is spin dependent.[16] If the gold is indeed magnetic, its direction of magnetization may affect the spin of the electrons or holes injected from the substrate into the chiral molecule and thereby affect the charge transfer rate through the chiral molecule. In the present study, we investigated electrochemically the charge transfer through a self-assembled monolayer of chiral oligopeptides with a terminal ferrocene group adsorbed on the gold substrate.

Several groups have reported an asymmetry in the charge transfer through short oligopeptides, which contain L-aminoacids and adopt an α-helix structure. Specifically, they noted that the rate constant for charge transfer from the electrode to the redox active group situated at the opposite end of the molecule is higher than the rate constant for transfer in the opposite sense.[17,18] This experimental observation was attributed to the relative orientation of the electrostatic field in the self-assembled monolayer (SAM) generated by the dipole moment of the oligopeptide itself with respect to the direction in which the charge carriers propagate. The electrostatic field generated by the dipole moment of the molecule is largely due to the close packing and parallel orientation of the molecules in the monolayer.[19]

While we were studying the rate constant for charge transfer through L- and D- oligopeptide monolayers by electrochemistry, we observed that the asymmetry in the charge transfer rate is opposite for the two enantiomers. Since the orientation of the dipole moment inside the monolayer is the same for the two enantiomers, the asymmetry cannot be related to the dipole moment orientation. We propose an explanation of the observed asymmetry based on the chiral induced spin selectivity (CISS) effect in the electron transfer[20] and the magnetization of the gold substrate.

We have studied by electrochemistry SAMs of D/L-12mer-Fc peptides (see structures in the Experimental Section). The cysteamine (Cya) situated at the C-end of the peptide was used for covalent binding to the gold electrode. The ferrocene (Fc) situated at the N-end of the peptide plays the role of electron donor or acceptor depending on the potential applied to the gold electrode. The circular dichroism (CD) spectra of a solution of the L-peptide show negative peaks at 208 and 222 nm and a positive peak at 192 nm, which are characteristic of a right-handed helix, while the D-peptide spectra show opposite peaks (**Figure 1**a). The θ_{222} nm/θ_{208} nm values reported in **Table 1** are indicative of both L- and D- peptides adopting a mixed $3_{10}/\alpha$ helical structure in solution.[19]

Dr. F. Tassinari, Dr. N. Kantor-Uriel, Dr. V. Varade, Prof. R. Naaman
Department of Chemical and Biological Physics
Weizmann Institute of Science
Rehovot 76100, Israel
E-mail: ron.naaman@weizmann.ac.il
Dr. D. R. Jayarathna, Prof. C. Achim
Department of Chemistry
Carnegie Mellon University
Pittsburgh, PA 15213, USA
Dr. K. L. Davis
Department of Chemistry
Manchester University
North Manchester, IN 46962, USA
The ORCID identification number(s) for the author(s) of this article can be found under https://doi.org/10.1002/adma.201706423.

DOI: 10.1002/adma.201706423

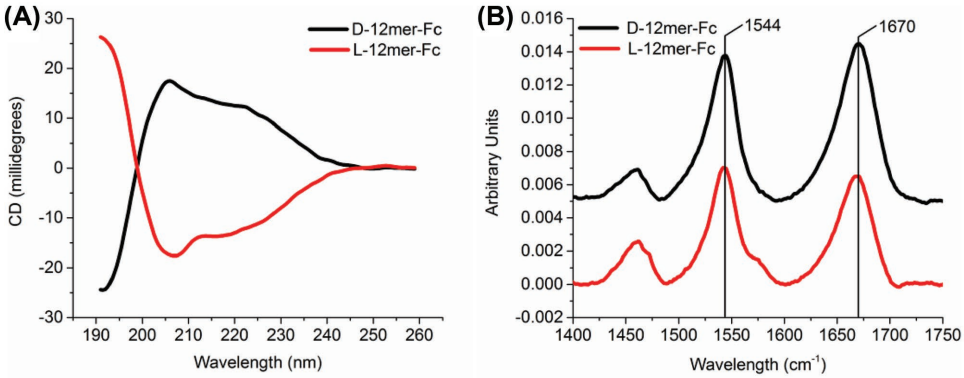

Figure 1. A) CD spectra for 0.1 mg mL^{-1} solutions of the D/L-12 mer-Fc in 1:1 (v/v) pH 7.0 10 mM sodium phosphate buffer : trifluoroethanol (TFE); B) The amide region of PMIRRAS spectra recorded for the self-assembled monolayers of L-12mer-Fc and D-12mer-Fc. The D-12mer-Fc spectrum is shifted up for clarity.

The polarization modulation–infrared reflection–absorption mode (PM–IRRAS) spectra of the adsorbed L- and D- peptides are identical in terms of both the position and the relative intensity of the amide I and II absorption bands observed at 1670 and 1544 cm^{-1}, respectively (Figure 1b). These bands are similar to the ones previously observed for SAMs of poly-L-alanine (1658 and 1545 cm^{-1})[21] and indicate that the two peptides adopt a α-helix structure in the self-assembled monolayer. The analysis of the electrochemistry data prove that the self-assembled monolayers of D/L-12mer-Fc peptides formed on gold have similar surface coverage (**Table 2**). The extracted tilt angle, γ, of the helix with respect to the surface normal is 48°, which is in good agreement to the reported value for similar systems.[16] Hence, the properties determined using PM-IRRAS and surface coverage indicate that the two peptide enantiomers form similar monolayers and adopt the same structure within these monolayers.

The calculated electron transfer rate constants for the D and L peptides (Table 2) are close to those previously reported for a polyalanine 14-mer.[16] **Figure 2** presents the experimental data compared to the theoretical curve for k_0 of 0.48 s^{-1}. For the D-peptide, the rate constant as determined by the analysis of the anodic process is larger than that determined by the analysis of the cathodic process. In contrast, for the L-peptide, the situation is reversed and the rate constant determined from the cathodic process is larger than that determined from the anodic process.

Several reasons have been suggested for the asymmetry in the rate constant for electron transfer through peptide monolayers, measured from the anodic and cathodic process: (1) The dipole moment of the helix may favor electron-transfer in the direction toward the positive end of the dipole;[16] (2) The amide-ferrocene strong electronic coupling promotes fast electron transfer[22] that would favor electron transfer between the C-terminal' amide group and the sulfur, which was being considered the rate-determining step; (3) the polarity of the Au-S junction defines a favorite direction for electron transfer.[17] These explanations cannot be used to rationalize the asymmetry observed for the two enantiomers we studied because the orientation and strength of the dipole moment, the amide-ferrocene electronic coupling, and the polarity of the Au-S junction do not depend on the chirality of the two peptides. This is also supported by the contact potential difference (CPD) measurements reported in **Table 3**, showing that the change of the work function of the Au surfaces after the monolayer formation is similar for the two enantiomers.

The model we propose to explain the observed asymmetry in the rate constant for the two peptides is based on two components, the magnetization of the system and the spin selective electron transfer through the chiral molecules. It was reported before that linking chromophores to a substrate via an organic monolayer may cause a large magnetic anisotropy in the sample.[23] Several groups already observed that binding paramagnetic molecules to gold through an organic linker causes spin selective conduction through the molecules.[15,24–26] Hence we propose, that as a result of the induced anisotropy, both the surface magnetization of the gold and the spin on the ferrocene are magnetized parallel to each other and along the axis of the molecule.

To verify this assumption, we measured the magnetization of the oligopeptide monolayer on gold at room temperature, using a superconducting quantum interference device (SQUID). **Figure 3** shows the magnetic moment as a function of the magnetic field applied either perpendicular or parallel to the surface. The results are presented after the subtraction of the contribution of the substrate without the monolayer.

Table 1. θ_{222} nm/θ_{208} nm and f_H percentage helix content of the peptides.

Peptide	θ_{222} nm/θ_{208} nm	f_H
D-12 mer Fc	0.75 ± 0.02	32 ± 1
L-12 mer Fc	0.71 ± 0.02	33 ± 1

Table 2. The electron transfer rate constants and surface coverage for the self-assembled monolayers of L/D-12mer-Fc.

	Surface coverage [mol cm^{-2}]	Rate constant oxidation [s^{-1}]	Rate constant reduction [s^{-1}]
L-12mer-Fc	3.6×10^{-11}	0.30 ± 0.02	0.47 ± 0.03
D-12mer-Fc	3.7×10^{-11}	0.48 ± 0.03	0.28 ± 0.03

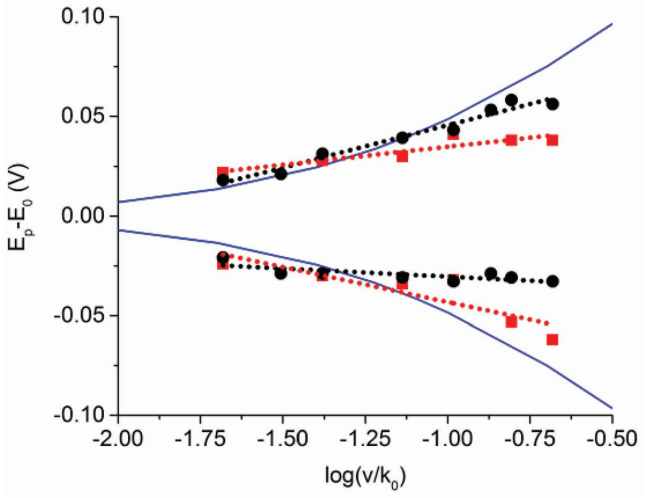

Figure 2. Plot of peak position relative to the formal potential (E_p–E_0) as a function of the normalized scan rate (ν/k_0) for either L-12mer-Fc (red squares) or D-12mer-Fc (black dots). The blue solid lines are calculated using the Marcus theory applying a standard electrochemical rate constant (k_0) of 0.48 s^{-1} and assuming the reorganization energy for the ferrocene to be 0.8 eV. The dotted lines are a guide for the eye.

A ferromagnetic response with a significant hysteresis is observed for both magnetic field directions. However, the response is nonisotropic. For the field applied perpendicular to the surface, the magnetic susceptibility is large and the hysteresis is about 40 Oe. For the magnetic field applied parallel to the surface, the magnetic susceptibility is somewhat smaller; however the hysteresis is much larger, namely 120 Oe. Assuming that the measured magnetic moment at H = 0 is proportional to the density of the monolayer, we calculated that the magnetic field per molecule is 0.86 μ_B for the parallel field and 0.64 μ_B for the perpendicular one. These two values are consistent with a SAM in which the molecules are at a tilt angle with respect to the surface normal of ≈50°, which is similar to the tilt angle inferred from the PM IRRAS (48°). Based on these results, we conclude that the easy axis of magnetization is along the molecular axis.

Identical results were obtained for the D-12mer-Fc monolayer (see the Supporting Information).

Table 3. Contact potential difference (CPD) of gold coated with SAM of oligopeptides.

	CPD [V]
Gold (blank)	0.0 ± 0.004
L-12mer-Fc monolayer	−0.539 ± 0.017
D-12mer-Fc monolayer	−0.486 ± 0.006

Our model for the rationalization of the enantio-dependent asymmetry in the electron transfer rate invokes spin-dependent electron transfer through the chiral molecules, an effect known as CISS.[16] The CISS has inherent asymmetry: for a given enantiomer, the preferred spin of electrons transferred in one direction is the opposite to that of electrons transferred in the opposite direction. In our system, we assume that both the gold substrate and the ferrocene have a magnetic moment parallel to each other and to the molecular axis (see **Figure 4**).

The electrons injected into the oligopeptide have therefore their spin oriented in the same direction, independent of them being transferred from the gold or from the ferrocene and independent on the specific enantiomer. However, because of the CISS effect, in the case of the L-peptide, the spin is oriented so that its transport is favored for the reduction direction while for the D-peptide it is favored for the oxidation direction.

To verify the model suggested above, we performed spin-dependent conduction studies with a conducting atomic force microscope (cAFM), using nickel/gold magnetic substrates for the monolayer formation. The current versus voltage was measured on the monolayer applying the magnetic field perpendicular to the substrate surface, pointing either up or down with respect to the surface. The potential is that of the Pt tip. The results shown in **Figure 5** indicate that the current through the monolayer depends strongly (typically a 4:1 ratio) on the direction of the magnetic field and implicitly on the spin orientation. It is also clear that when the magnetic field is pointing up, the reduction (positive voltage) is favored over oxidation (negative voltage) for the L enantiomer, while when the field is pointing down, the oxidation is favored for the D enantiomer. Thus, the spin-dependent transport studies corroborate the importance of spontaneous

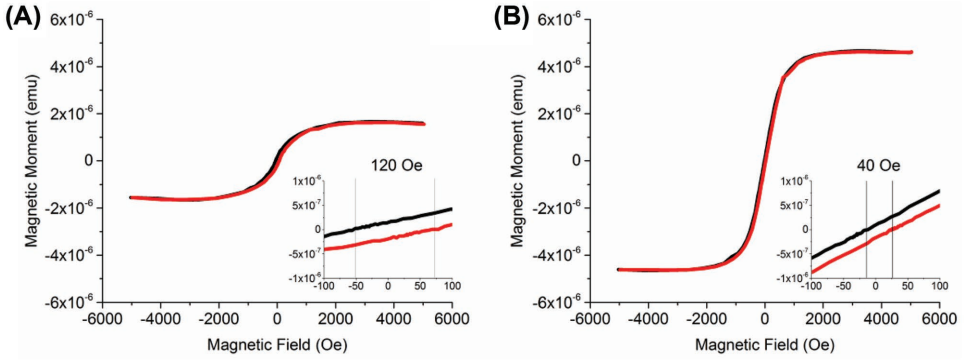

Figure 3. Magnetic moment versus magnetic field measured by SQUID at 300 K for the L-12mer-Fc monolayer adsorbed on gold film. The substrate contribution to the signal has been subtracted from the data. The magnetic field was applied either parallel A) or perpendicular B) to the sample surface. The inset is a zoom of the low field region where the hysteresis is largest.

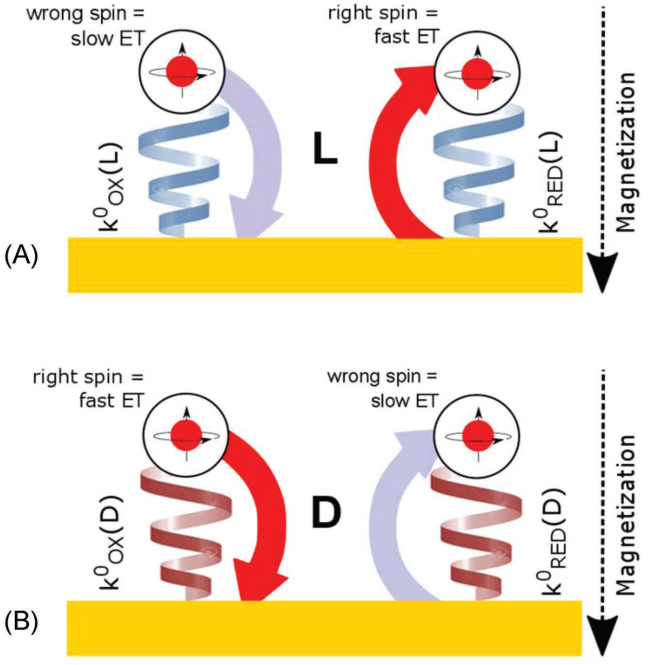

Figure 4. A scheme of the proposed mechanism for the asymmetric electron transfer. The gold is magnetized. As a result, one spin is injected preferentially from it to the molecule or vice versa. A) In the case of L-oligopeptide (right handed helix) the electron injected from the gold has a spin aligned parallel to the electron's velocity, which is the preferred spin for the electron transfer. As a result, the electron transfer in this direction (reduction process) is faster than backward. B) In the case of D-oligopeptide (left handed helix), the preferred spin orientation is antiparallel to the electron's velocity; therefore the preferred rate is for the oxidation process.

magnetization of the system as well as the spin selectivity in the electron transfer.

This work is an example for "spontaneous magnetization" that affects the charge transfer rates in chiral molecules. The observations presented here are consistent with the asymmetry in electron transfer observed in previous studies.[17,18] However, because of our ability to probe both enantiomers the mechanism for the process was revealed. Since in Nature paramagnetic ions are abundant in proteins and since proteins are chiral, similar effects may be relevant also in biological systems.

Experimental Section

Peptide Synthesis: The sequence of the peptides was designed with the goal that the peptides (1) were as short as possible to make the synthesis simple and (2) adopted a helical structure. The D/L-12mer peptides Cya-(D/L-ala)$_3$-aib-(D/L-ala)$_2$-aib-(D/L-ala)$_2$-aib-(D/L-ala)$_2$ (cya = cysteamine; ala = alanine; aib = aminoisobutyric acid) satisfy these requirements.[27,28] The incorporation of 2-amino isobutyric acid into the sequence makes the peptides more hydrophilic and quite soluble when compared to, for example, polyalanine. This in turn made the purification of the peptides by reverse phase high pressure liquid chromatography (HPLC) relatively simple. D/L-12mer-Fc peptides were synthesized manually using Fmoc-solid phase peptide synthesis strategy, starting form commercially available cysteamine-4-methoxytrityl resin with a loading of ≈0.83 meq g^{-1} (Anaspec). Fmoc-D/L-alanine(ala)-OH (Anaspec) was coupled using 1-[bis(dimethylamino)methylene]-1H-1,2,3-triazolo[4,5-b]pyridinium 3-oxid hexafluorophosphate (HATU, Chem-Impex) as coupling reagent. 6-Chloro-benzotriazole-1-yloxy-tris-pyrrolidinophosphonium hexafluorophosphate (PyClock: Peptides International) was used as the coupling of Fmoc-2-aminoisobutyric acid (aib)-OH (Anaspec). 2-(1*H*-benzotriazol-1-yl)-1,1,3,3-tetramethyluronium hexafluorophosphate (HBTU: Chem-Impex) was used as the coupling reagent for ferrocene carboxylic acid (Sigma-Aldrich). Anhydrous *N*,*N*′-diisopropylethylamine and anhydrous *N*-methyl-2-pyrrolidone (Sigma-Aldrich) were used as the base and the solvent, respectively. The success of coupling of each amino acid was monitored by qualitative Kaiser test. The peptides were cleaved from the resin with a cleavage cocktail of 95% trifluoroacetic acid (EMD), 2.5% triisopropylsilane (Sigma-Aldrich), 2.5% water, and two drops of immobilized tris(2-carboxyethyl)phosphine disulfide reducing gel (Thermo Scientific). Crude peptides were precipitated with cold diethyl ether (EMD) and dried under nitrogen. Peptides were purified by reversed-phase HPLC using a C18 silica column on a Waters 600 controller and pump. Absorbance was monitored with a Waters 2996 photodiode array detector. The peptides have been characterized

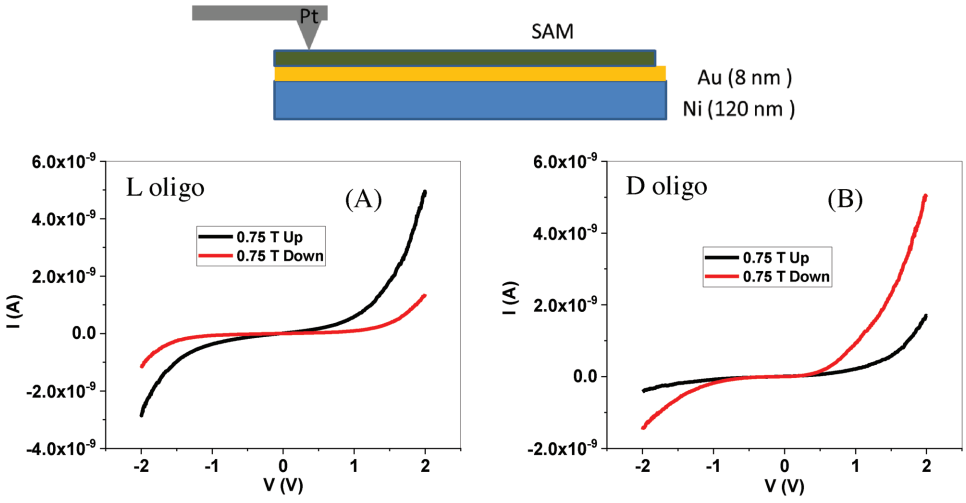

Figure 5. Spin dependent conduction through monolayers made from L-12mer-Fc or D-12mer-Fc molecules. The system is presented schematically in the upper scheme. The current versus voltage is presented for the L and D oligomers A) and B), respectively. While for the L enantiomer the current is higher when the Ni magnet is pointing up, for the D enantiomer it is higher for the magnet pointing down.

by electron spray ionization-mass spectroscopy. Calc/exp: D-12mer-Fc 1184.2/1184.2 and L-12mer-Fc 1184.2/1184.2 (see Figure S1, Supporting Information). Samples of the lyophilized D/L-12mer-Fc were dissolved in a 1:1 (v/v) mixture of TFE : nanopure water.

CD Spectroscopy: The CD spectra for the peptides were measured in 1:1 (v/v) mixture of pH 7.0 10 mM sodium phosphate buffer and TFE, in 0.1 cm path length cuvettes, at 20 °C on a JASCO J-715 spectrometer equipped with a thermoelectrically controlled single-cell holder. The scan rate was 100 nm min^{-1} and 10 scans were accumulated for each spectrum. The concentration of the peptides was 0.1 mg mL^{-1}. The helix content of the peptides was determined from the CD data using the equations[29]

$$f_H = -\frac{[\theta]_{222} + 2340}{30300} \quad (1)$$

where $[\theta]_{222}$ is the mean residue ellipticity at 222 nm, and f_H is the fraction of helix (both α and 3_{10})

$$[\theta]_{222}\ (\text{deg cm}^2\ \text{dmol}^{-1}) = \theta_{222} \times M / [10 \times d \times C \times (N-1)] \quad (2)$$

where θ_{222} is the observed ellipticity in degrees at 222 nm, M is the molecular weight of the peptide, d is the path length in cm, C is the concentration in g mL^{-1}, and N is the number of peptide bonds in the peptide.[30]

Monolayer Formation: For the samples used in the electrochemistry experiments and the characterizations, the 120 nm thick gold surfaces were prepared by e-beam evaporation on a p-doped silicon wafer, using 3 nm of chromium as the adhesion layer. For the samples used in the SQUID measurements, 8 nm of titanium instead of 3 nm of chromium were used as the adhesion layer, to avoid the complications to the measurements arising from the magnetic properties of chromium. For the samples used in the magnetic AFM measurements (m-AFM), the surfaces were prepared by sputtering 120 nm of nickel, followed by a 8 nm thick gold layer on top of a silicon wafer with a 2 µm thermal silicon oxide layer, with a 8 nm titanium as the adhesion layer. The use of the Ni/Au surfaces for the mAFM measurements was necessary in order to be able to spin-polarize the electrons injected from the surface using an external magnetic field. All the surfaces were cleaned by boiling them first in acetone and then in ethanol for 10 min, followed by a UV-ozone cleaning for 15 min and a final incubation in warm ethanol for 40 min.

The surfaces, dried with a nitrogen gun, where immediately immersed into the peptide solution (0.625 mg mL^{-1}, using a 1:1 mixture of pH 7.0 10 mM sodium phosphate buffer and TFE) and incubated for 36 h. After the incubation, the surfaces were rinsed 3 times with deionized water, dried with a nitrogen gun, and immediately used for the experiments. The monolayers were characterized by AFM measurements (see the Supporting Information) as well as by IR spectroscopy, CPD studies, SQUID measurements, and cyclic voltammetries.

PM-IRRAS: Infrared spectra were recorded using a Nicolet 6700 FTIR instrument equipped with a PEM-90 photoelastic modulator (Hinds Instruments, Hillsboro, OR) at an 80° angle of incidence. The orientation of the peptides on the gold surface was determined using the following equation[31]

$$\frac{I_1}{I_2} = 1.5 \times \left[\frac{(3\cos^2\gamma - 1)(3\cos^2\theta_1 - 1) + 2}{(3\cos^2\gamma - 1)(3\cos^2\theta_2 - 1) + 2}\right] \quad (3)$$

where I_1 and I_2 are the intensity of the amide I and amide II bands, θ_1 and θ_2 are the angles between the transition moment of the two bonds and the helical axis (which were found in the literature to be 39° and 75°, respectively[32]) and γ is the tilt angle of the helix in respect to the surface normal.

Electrochemistry: The electrochemical experiments consisted in cyclic voltammetry experiments carried out at different scan rates (ν) ranging from 10 to 100 mV s^{-1} in a potential window from 0.0 to 0.7 V, using the oligopeptide modified gold surface as working electrode.

The measurements were done using a standard three-electrode setup, in a supporting electrolyte solution of 0.1 M $NaClO_4$, using a Pt wire as the counter electrode and a Ag/AgCl (sat. KCl) electrode as reference. The instrument was an Autolab PGSTAT 20 potentiostat. Following the same approach used by Waldeck and co-workers,[33] the charge transfer rate constant k^0 was obtained from the experimental data by plotting the anodic and cathodic peak separation (E_p–E_0) versus the normalized scan rate (ν/k^0) and fitting the data by a curve obtained by Marcus theory, using a recombination energy (λ) of 0.8 eV for the ferrocene.

The surface coverage Γ was calculated by integrating the charge under the faradaic current peaks at a scan rate of 50 mV s^{-1}.

Contact Potential Difference: The CPD of the surfaces was determined using a commercial Kelvin probe instrument (Delta Phi Besocke, Jülich, Germany) within a Faraday cage. The reference probe consisted of a gold grid. The measurements were held in the dark and in ambient atmosphere. The CPD signal of a blank gold substrate was taken as the zero value. The CPD of the monolayers is reported as the difference between the gold reference and the value recorded for the monolayers after letting the signal stabilize. The results are summarized in Table 3.

SQUID Measurements: The magnetic properties were measured using a SQUID (superconducting quantum interference device) magnetometer MPMS3 (L.O.T.- Quantum Design inc.) with the magnetic field applied either parallel or perpendicular to the sample plane. The vibrating sample magnetometry was in use. The measurements were conducted at 300 K, and consisted in a magnetizing run from 0 to 5000 Oe, a first measurement going from 5000 to –5000 Oe, a second going from –5000 to 5000 Oe, and a demagnetizing run from 5000 to 0 Oe. The diamagnetic contribution of the gold-titanium-silicon substrate was measured prior to the monolayer formation and subtracted from the final data.

Supporting Information

Supporting Information is available from the Wiley Online Library or from the author.

Acknowledgements

R.N. acknowledges the support from the Israel Science Foundation and by the European Research Council under the European Union's Seventh Framework Program (No. FP7/2007-2013)/ERC grant Agreement No. 338720 CISS and by the Templeton Foundation. C.A. acknowledges financial support from the US NSF (No. CHE-1413202) and interesting discussions with Dr. Yossi Paltiel. The authors acknowledge the help of Dr. Gregory Leitus with the measurements of the magnetic properties of the samples and Dr. Davide Ceratti for helpful discussions.

Conflict of Interest

The authors declare no conflict of interest.

Keywords

chirality, electron transfer, magnetization, self-assembled monolayers, spin

Received: November 4, 2017
Revised: February 19, 2018
Published online: April 2, 2018

[1] A. B. Marciel, M. Tanyeri, B. D. Wall, J. D. Tovar, C. M. Schroeder, W. L. Wilson, *Adv. Mater.* **2013**, *25*, 6398.
[2] J. I. N. Oliveira, E. L. Albuquerque, U. L. Fulco, P. W. Mauriz, R. G. Sarmento, *Chem. Phys. Lett.* **2014**, *612*, 14.
[3] C. E. D. Chidsey, *Science* **1991**, *251*, 919.
[4] M. M. Galka, H. B. Kraatz, *ChemPhysChem* **2002**, *3*, 356.
[5] M. Kettner, B. Göhler, H. Zacharias, D. Mishra, V. Kiran, R. Naaman, C. Fontanesi, D. H. Waldeck, S. Sęk, J. Pawłowski, J. Juhaniewicz, *J. Phys. Chem. C* **2015**, *119*, 14542.
[6] H. S. Kato, Y. Murakami, Y. Kiriyama, R. Saitoh, T. Ueba, T. Yamada, Y. Ie, Y. Aso, T. Munakata, *J. Phys. Chem. C* **2015**, *119*, 7400.
[7] A. L. Eckermann, D. J. Feld, J. A. Shaw, T. J. Meade, *Coord. Chem. Rev.* **2010**, *254*, 1769.
[8] I. Carmeli, G. Leitus, R. Naaman, S. Reich, Z. Vager, *J. Chem. Phys.* **2003**, *118*, 10372.
[9] P. Crespo, R. Litrán, T. C. Rojas, M. Multigner, J. M. de la Fuente, J. C. Sánchez-López, M. A. García, A. Hernando, S. Penadés, A. Fernández, *Phys. Rev. Lett.* **2004**, *93*, 087204.
[10] S. Trudel, *Gold Bull.* **2011**, *44*, 3.
[11] R. Singh, *J. Magn. Magn. Mater.* **2013**, *346*, 58.
[12] G. L. Nealon, B. Donnio, R. Greget, J. P. Kappler, E. Terazzi, J. L. Gallani, *Nanoscale* **2012**, *4*, 5244.
[13] M. Agrachev, S. Antonello, T. Dainese, M. Ruzzi, A. Zoleo, E. Aprà, N. Govind, A. Fortunelli, L. Sementa, F. Maran, *ACS Omega* **2017**, *2*, 2607.
[14] M. Suzuki, N. Kawamura, H. Miyagawa, J. S. Garitaonandia, Y. Yamamoto, H. Hori, *Phys. Rev. Lett.* **2012**, *108*, 047201.
[15] A. C. Aragonès, D. Aravena, J. I. Cerdá, Z. Acís-Castillo, H. Li, J. A. Real, F. Sanz, J. Hihath, E. Ruiz, I. Díez-Pérez, *Nano Lett.* **2016**, *16*, 218.
[16] R. Naaman, D. H. Waldeck, *Ann. Rev. Phys. Chem.* **2015**, *66*, 263.
[17] S. Sek, A. Tolak, A. Misicka, B. Palys, R. Bilewicz, *J. Phys. Chem. B* **2005**, *109*, 18433.
[18] M. Venanzi, E. Gatto, M. Caruso, A. Porchetta, F. Formaggio, C. Toniolo, *J. Phys. Chem. A* **2014**, *118*, 6674.
[19] V. S. Lvov, R. Naaman, Z. Vager, V. Tiberkevich, *Chem. Phys. Lett.* **2003**, *381*, 650.
[20] K. Michaeli, N. Kantor-Uriel, R. Naaman, D. H. Waldeck, *Chem. Soc. Rev.* **2016**, *45*, 6478.
[21] S. Krimm, J. Bandekar, *Adv. Protein Chem.* **1986**, *38*, 181.
[22] J. Watanabe, T. Morita, S. Kimura, *J. Phys. Chem. B* **2005**, *109*, 14416.
[23] A. Zakrassov, A. Bitler, L. Etgar, G. Leitus, E. Lifshitz, R. Naaman, *Phys. Chem. Chem. Phys.* **2009**, *11*, 7549.
[24] A. Hernando, P. Crespo, M. A. Garcıá, *Phys. Rev. Lett.* **2006**, *96*, 057206.
[25] J. M. D. Coey, M. Venkatesan, C. B. Fitzgerald, A. P. Douvalis, I. S. Sanders, *Nature* **2002**, *420*, 156.
[26] T. L. Makarova, *Semiconductors* **2004**, *38*, 615.
[27] C. Tonlolo, E. Benedetti, *Trends Biochem. Sci.* **1991**, *16*, 350.
[28] S. Bezer, M. Matsumoto, M. W. Lodewyk, S. J. Lee, D. J. Tantillo, M. R. Gagné, M. L. Waters, *Org. Biomol. Chem.* **2014**, *12*, 1488.
[29] Y. H. Chen, J. T. Yang, H. M. Martinez, *Biochemistry* **1972**, *11*, 4120.
[30] C. Toniolo, A. Polese, F. Formaggio, M. Crisma, J. Kamphuis, *J. Am. Chem. Soc.* **1996**, *118*, 2744.
[31] D. E. López-Pérez, G. Revilla-López, D. Jacquemin, D. Zanuy, B. Palys, S. Sek, C. Alemán, *Phys. Chem. Chem. Phys.* **2012**, *14*, 10332.
[32] Y. Miura, S. Kimura, Y. Imanishi, J. Umemura, *Langmuir* **1998**, *14*, 6935.
[33] E. Wierzbinski, A. de Leon, K. L. Davis, S. Bezer, M. A. Wolak, M. J. Kofke, R. Schlaf, C. Achim, D. H. Waldeck, *Langmuir* **2012**, *28*, 1971.

